Online Evaluation for Chance-Constrained Geofences under Data-Driven Uncertainties

Pengcheng Wu*
University of California San Diego, La Jolla, CA, 92093
San Diego State University, San Diego, CA, 92182

Jun Chen†
San Diego State University, San Diego, CA, 92182

Urban air mobility (UAM) using electrical vertical take-off and landing (eVTOL) aircraft is an emerging way of air transportation within metropolitan areas. A key challenge for the success of UAM is how to manage large-scale flight operations with safety guarantee in high-density, dynamic and uncertain airspace environments in real time. To deal with these challenges, in this paper we combine the concept of geofence and chance constraints to obtain chance-constrained geofences under data-driven uncertainties, which can guarantee that the probability of potential conflicts between eVTOL aircraft is bounded given a general empirical distribution. To evaluate the chance-constrained geofences in an online fashion, Kernel Density Estimation (KDE) based on Fast Fourier Transform (FFT) is adopted and customized to model data-driven uncertainties. Comprehensive numerical simulations demonstrate the feasibility and efficiency of the online evaluation of chance-constrained geofence through the algorithm of FFT-based KDE.

I. Introduction

A. Motivation

The applications of urban air mobility (UAM) are increasingly drawing great attention from many institutes such as NASA, the Federal Aviation Administration (FAA), and airlines [1], [2]. The vision of UAM is to use revolutionary electrical vertical take-off and landing (eVTOL) aircraft to provide efficient and on-demand air transportation service between places previously underserved by the current aviation market. Companies such as Airbus, Boeing, Bell, Joby, Archer, Lilium, and Aurora Flight Sciences are competing to build and test their newly designed eVTOL aircraft [3], [4]. To well serve a significant proportion of urban transportation demand, UAM will introduce a large number of eVTOL aircraft in the limited urban airspace [5], [6], where the environment is also highly uncertain due to inaccurate localization with disturbances from high buildings, such as strong Global Positioning System (GPS) [7] noise and high wind disturbance around those buildings. Therefore, a key challenge for the success of UAM is how to ensure operation safety in high-density, dynamic and uncertain airspace environments in real time. This paper will introduce a concept called chance-constrained Geo-fences which can guarantee that the probability of potential conflicts is bounded and low. To efficiently evaluate the chance-constrained Geo-fences in an online fashion, a data-driven method is developed for any general empirical distribution.

B. Related work

As numerous eVTOL aircraft are permitted to enter the airspace, the airspace will become congested, which surpasses the capacity of the current air traffic control system. To address this issue, capable UAM Traffic Management (UTM) will be needed to manage UAM traffic. A key component of UTM is the presence of geofences, reserving airspace volumes as a practical alternative to strictly route-based reservations [8]. The airspace is partitioned into usable airspace and no fly zones through the introduction of geofences. To enforce geofence boundaries, a geofence system monitors the positions of eVTOL aircraft with respect to geofence boundaries, determines whether the eVTOL aircraft is violating the geofence, and responds according to the status of geofence violation. Currently, many researches on UAM are proposed based on structured airspace, where static geofences are specified and the eVTOL aircraft need to

*Joint PhD Student, Department of Aerospace Engineering, Student Member AIAA, pwu@sdsu.edu,pcwupat@ucsd.edu
†Assistant Professor, Department of Aerospace Engineering, Member AIAA, jun.chen@sdsu.edu

follow the fixed routes inside the geofences for conservative safety concerns [9]. This is a safe way but not efficient for UAM because the traffic density of UAM will be quite high. To increase the airspace's capacity, the FAA and NASA are investigating the free-flight airspace framework with trajectory-based operations [10], which can handle higher air traffic density even in uncertain environments [11]. Without the protection of structured airway, aircraft need to rely on accurate localization provided by navigation technologies such as Automatic Dependence Surveillance-Broadcast (ADSB) and GPS [7]. Thus the location uncertainty or error of an aircraft is a critical issue to ensure safety.

Ideally, for safe and reliable flying, the requirement of collision avoidance should be realized. However, various kinds of uncertainty may be present in realistic scenarios, which may highly increase the chance of infeasibility for operations based on the current collision avoidance system. Under this circumstance, it is impossible to find a guaranteed-feasible solution. Alternatively, we can switch to identify trajectories which ensure the probability of conflict occurrence is within a prescribed bound if following such trajectories [12]. Thus, accounting for the knowledge of uncertainty in path planning is regarded as an essential step to achieve safety assurance. In [13], a probabilistic map is constructed using a likelihood function and a safe UAV path is then generated by solving a probability minimization problem. In [14], [15], the sampling-based Monte Carlo method is accurate enough to estimate conflicts between aircraft stochastically, but it sacrifices computation efficiency since it takes much computation time to figure out the probability of conflict occurrence. To achieve the balance between planning conservatism and efficiency, the stochastic constraints can be reformulated as tightened deterministic constraints through chance constraints formulation [16], [17]. Blackmore et al. [18], [19] proposed chance-constrained programming model to consider various uncertainties for conflict avoidance problem, but such formulations are often computationally expensive, which may scale poorly as the dimensions of configuration spaces increase. Wu et al. [20] present a chance-constrained algorithm CCRRT which uses sampling-based methods to identify paths for linear systems subject to uncertainty. Sampling-based algorithms like CCRRT scale well because they perform trajectory-wise constraint checking [21]. However, all the aforementioned works adopt the assumption that the uncertainty obeys Gaussian distribution, which may not be consistent with the engineering practice [22], [23].

C. Contributions and structure

In this paper, we will combine the concept of geofence and chance constraints to present a way of online data-driven evaluation to capture chance-constrained geofence. On the one hand, the captured chance-constrained geofence can guarantee that without violating the geofence, the probability of potential conflicts between eVTOL aircraft in UAM is within a bound. Compared with the existing works which evaluate chance constraints by assuming Gaussian uncertainties, our proposed method applies to general data-driven distributions, not limited to Gaussian distributions. On the other hand, the data-driven distribution is based on online sampled data points of location, so the distribution is also updating with more data samples coming in. This poses a great challenge to deal with data-driven distributions in real time. Through the implementation of Fast Fourier Transform (FFT) algorithm to speed up the computation of Kernel Density Estimation (KDE), the proposed method can reduce time-consuming evaluations and thus make real time computation feasible.

The major contributions of this paper are highlighted as follows:

1) To model high-dimensional data-driven distributions through online data samplings, FFT is encoded into traditional KDE to greatly accelerate the computation. Although most kernel estimators can use KDE to approximate probability density function (PDF) of the data-driven distribution, the direct approach to evaluate KDE can be computationally expensive, especially when the number of data samplings becomes very large [24]. Instead, we present an alternative way to replace performing kernel evaluation on data points by that on grids. Further, FFT can be implemented to reduce computational complexity owing to the structure of discrete convolution of kernel evaluation. Numerical study shows this indirect approach can dramatically increase the speed of computation.

2) According to the results of KDE evaluation, a search method is developed to identify the chance-constrained geofence for the data-driven distributions, not limited to Gaussian distributions, at any confidence level. The identification of chance-constrained geofence can help translate the data-driven uncertainty into deterministic constraints for the path planning of eVTOL aircraft in UAM applications. Numerical study demonstrates the evaluation of chance-constrained geofence can be achieved in an online fashion.

The content of the paper is organized as follows: in Section II, we are going to formally set up the problem and define the chance-constrained geofences; in Section III, we will develop an online computational algorithm to capture the chance-constrained geofences; in Section IV, we will conduct some numerical simulations to verify the feasibility and efficiency of the proposed algorithm; last but not least, we will conclude this paper in Section V.

II. Problem Formulation

For an eVTOL in UAM, its location $\boldsymbol{x}_t$ at a particular time t may be stochastic, due to uncertainty arising from the inaccurate sensor of self-position or environmental disturbance like wind. We can assume that the location $\boldsymbol{x}_t$ obeys a data-driven distribution.

To operate safely in a dynamic environment, each eVTOL should try to avoid conflicts with other eVTOLs in the system. This can be achieved by introducing the following constraints

$$\begin{aligned} &\boldsymbol{x}_t \notin \mathcal{X}_t \quad \forall t \\ &\text{where } \mathcal{X}_t := (\bigcup_{i=1}^{n} \mathcal{X}_{ti}) \end{aligned} \tag{1}$$

In the above constraints, we use $\mathcal{X}_{ti}$ to denote the area in which aircraft i may be located at time t due to aircraft location uncertainty, where $i \in \{1, 2, \ldots, n\}$ and n is the total number of all the other aircraft. We call such a region as the possible region for all the other aircraft i at time t. Note that, from the perspective of a particular aircraft, all the other aircraft in the system actually can be viewed as obstacles to avoid. The time dependence of $\mathcal{X}_{ti}$ allows the inclusion of either static or dynamic obstacles. In this paper, for a particular aircraft in the system, all the other aircraft need to be treated as dynamic ones.

From the perspective of a particular aircraft, the possible region of another aircraft i at time step t can be modeled by the following equation

$$\mathcal{X}_{ti} = \{\boldsymbol{x} \in \mathbb{R}^d \mid \|\boldsymbol{x} - \boldsymbol{c}_{ti}\| \leq r_i\} \quad \forall t, i. \tag{2}$$

where r_i is the minimum safety range for the particular aircraft to stay away from the ith aircraft to ensure safety. In addition, $\boldsymbol{c}_{ti}$ represents the position of the ith aircraft at time t, which obeys the data-driven distribution.

We hope that the probability of collision between any two aircraft in the system at any time is less than a certain threshold, i.e.,

$$\Pr(\text{collision}) \leq 1 - \alpha \tag{3}$$

where α is the confidence level of the data-driven distribution.

We aim to quantify the probability of an aircraft to avoid conflicts with other aircraft considering location uncertainty as presented in eq. (3). To realize this goal, we can define the chance-constrained geofence $\mathcal{D}$ as

Definition **(Chance-Constrained Geofence)** A set $\mathcal{D} \subset \mathbb{R}^d$ that satisfies

$$\Pr(\boldsymbol{X} \in \mathcal{D}) \geq \alpha \tag{4}$$

is called a chance-constrained geofence at confidence level α of a random variable $\boldsymbol{X}$ which obeys a data-driven distribution.

Accordingly, we can convert the possible region $\mathcal{X}_{ti}$ introduced in eq. (2) into a chance-constrained geofence $\mathcal{D}$ at a given confidence level α. The task of this paper is to quantitatively identify the chance-constrained geofence for a data-driven distribution at any confidence level α.

III. Online Evaluation of Chance-Constrained Geofence

In this section, we are going to develop an online algorithm to capture the chance-constrained geofence defined in last section. Kernel Density Estimation (KDE) is a classical way to handle data-driven distributions, we can directly perform evaluations to figure out KDE values based on all samples. However, a significant issue that arises in the practice of traditional KDE is its computational intensity, the direct KDE approach runs slowly because it needs to have a kernel on every data point. Alternatively, we will present a way to speed up the computation of KDE at the cost of replacing kernel estimators by their approximations. The essential idea behind the operation is to perform kernel estimators on the grid points instead of the sampled data points. Further, the algorithm of FFT can be integrated to speed up the computation of discrete convolution to evaluate KDE values. This proposed method applies to any d-dimensional data-driven distributions.

A. Traditional kernel density estimator

A traditional method of KDE can be formulated through placing a kernel function $K(\cdot)$ on every data point x_i

$$\hat{f}(x) = \frac{1}{N}\sum_{i=1}^{N} K(x - x_i) \tag{5}$$

where N represents the number of data points.

Taking the bandwidth h of $\hat{f}(x)$ into consideration and assigning different weights w_i to different data points x_i, eq. (5) can be rewritten as

$$\hat{f}(x) = \frac{1}{h}\sum_{i=1}^{N} w_i K\left(\frac{x - x_i}{h}\right) \tag{6}$$

where $\sum_{i=1}^{N} w_i = 1$.

The discretized form of traditional KDE can be obtained through evaluating the values of KDE over a mesh composed of M grid points $g_1, \ldots, g_M$ in each dimension

$$\hat{f}_j = \frac{1}{h}\sum_{i=1}^{N} w_i K\left(\frac{g_j - x_i}{h}\right),\ j = 1, \ldots, M \tag{7}$$

An extension of eq. (6) to d-dimensional scenarios is to write

$$\hat{f}(x) = h^{-1}\sum_{i=1}^{N} w_i K\left(h^{-1}(x - x_i)\right) \tag{8}$$

where $\sum_{i=1}^{N} w_i = 1$, and $K(\cdot)$ is a d-variate kernel function. Also, its discretized form can be derived as

$$\hat{f}_j = h^{-1}\sum_{i=1}^{N} w_i K\left(h^{-1}(g_j - x_i)\right),\ j = 1, \ldots, M \tag{9}$$

For simplicity, eq. (8) and eq. (9) can be denoted as the following form

$$\hat{f}(x) = \sum_{i=1}^{N} w_i K_h\left(x - x_i\right), \quad \hat{f}_j = \sum_{i=1}^{N} w_i K_h\left(g_j - x_i\right),\ j = 1, \ldots, M \tag{10}$$

B. Online identification of chance-constrained geofence

The computational intensity of traditional KDE is very high. Instead of direct evaluation, we can go through N data points and assign weights to M equidistant grid points [25]. To speed up the evaluation of traditional KDE, the kernel function $K(\cdot)$ performed on N data points x_i can be replaced by that on M grid points g_l.

The idea is to go through every data point and then assign weights to its neighbour grid points. We need to obtain the grid weights c_l. The weights are determined by the proportion of the volume of a hyper-cube that is enclosed by the data point. For bi-variate kernel estimators, as shown in fig. 1, the mass associated with the data point X is distributed among each of the four surrounding grid points according to areas of the opposite sub-rectangles induced by the position of the data point. By doing so, we can obtain the approximation of eq. (9)

$$\hat{f}_j = \sum_{l=1}^{M} K_h\left(g_j - g_l\right) c_l,\ j = 1, \ldots, M \tag{11}$$

where $c_l, l = 1, \ldots, M$ are the grid weights assigned to every grid point g_l, which is determined by the amount of data points x_i in the neighbourhood of g_l. In this way, the number of kernel evaluations is only $O(M)$, which greatly saves running time, especially for large samples of data points.

Further, let $L = M - 1$ and then eq. (11) can be reformulated as

$$\hat{f}_j = \sum_{l=-L}^{L} c_{j-l} k_l, \ j = 1, \ldots, M \tag{12}$$

where

$$k_l = K_h \left(g_j - g_l \right) \tag{13}$$

Note that $c_l = 0$ for l not in the index set $\{1, \ldots, M\}$. By the symmetry of the kernel function $K_h(\cdot)$, it's only required to figure out k_l for $l = 0, 1, \ldots, L$ where $L = M - 1$. Therefore, it is clear that no more than M kernel evaluations are required to obtain k_l. This is because there are only M distinct differences among different grid points. Indeed, eq. (12) can be viewed as the discrete convolution of c_l and k_l. This means the approximation we use has a discrete convolution structure which can be computed quickly using FFT. Let C and K be the discrete Fourier transform of c_l and k_l respectively using FFT, and let F be the element-wise product of C and K. Then the values of KDE $\hat{f}_j$ can be extracted from the inverse FFT of F. By doing so, we can obtain KDE which approximates PDF function of the data-driven distribution in real time.

There are two roles that grid points play in this process: the KDE function is evaluated on grid points; grid weights c_l are assigned to every grid point.

After obtaining KDE values, we can identify chance-constrained geofence at any confidence level α for the data-driven distribution. Without violating the identified geofence, the probability of potential conflicts between eVTOL aircraft in UAM is within the bound $1 - \alpha$.

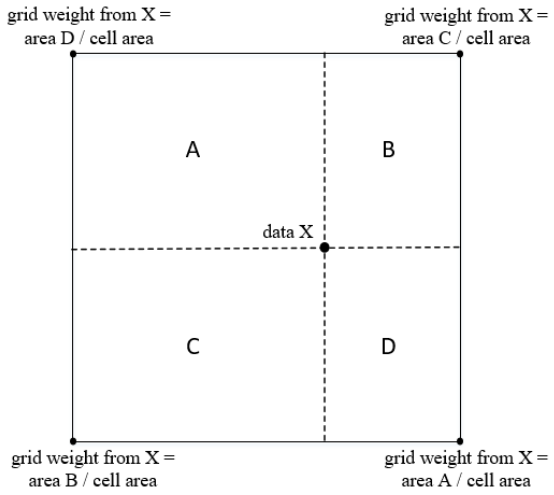

Fig. 1 Diagram of assigning weights to grid points [24]

C. Online evaluation algorithm

The details of the proposed algorithm are stated in **Algorithm 1**.

In the pseudo codes, N is the number of sampled data points. M is the number of grid points in each dimension. α represents the confidence level of the data-driven distribution. ϵ represents the error of threshold. In Line 9 and 10, FFT is employed to speed up the computation of discrete convolution to obtain KDE values. In Line 20, the chance-constrained geofence at the confidence level α of the data-driven distribution can be returned if successfully identified.

In summary, we present an alternative way to replace performing kernel evaluation on data points by that on grids. Further, FFT can be implemented to reduce computational complexity owing to the structure of discrete convolution of kernel evaluation. Based on the results of KDE evaluation, we propose an algorithm of online data-driven evaluation to capture chance-constrained geofence. The identification of chance-constrained geofence can help translate the data-driven uncertainty into deterministic constraints for the path planning of eVTOL aircraft in UAM applications.

Algorithm 1 Online Evaluation of Chance-Constrained Geofence

function DataGenerate(N)
    generate N data points randomly
    return $data$

function KernelDensityEstimator($data$, M, α)
    mesh with M grid points in each dimension
    obtain grid weights c_l according to $data$
    evaluate kernel functions k_l on grids
    C = FFT(c_l); K = FFT(k_l)
    kde = iFFT($C * K$)
    return kde

function GeofenceSearch(kde, α)
    low = min(kde); $high$ = max(kde)
    while $low < high$ **do**
        $mid = (low + high)/2$
        $geofence = (kde > mid)$
        Pr = sum($geofence$) / sum(kde)
        if $| Pr - \alpha | < \epsilon$ **then**
            return $geofence$
        else
            if $Pr < \alpha$ **then**
                $high = mid$
            else
                $low = mid$
    return $Failure$

IV. Numerical Study

A. Test settings

In this section, we are going to capture the chance-constrained geofence of a given bi-modal distribution using the algorithm of Online Evaluation of Chance-Constrained Geofence. Numerous data points are sampled obeying the bi-modal distribution. There are several crucial parameters which can impact the performance of the proposed algorithm: the number of data points N, the number of grid points in each dimension M, and the confidence level α. The tests were implemented in Python 3.8 and on an Intel(R) Core(TM) i5-8400T 1.70GHz PC with 8GB RAM.

B. Impact of confidence levels

In this part, tests are conducted under three different confidence levels: $\alpha = 80\%$, $\alpha = 90\%$, and $\alpha = 95\%$. The number of data points $N = 10^4$ and grid points $M = 128 * 128$.

1) Confidence level $\alpha = 80\%$

The chance-constrained geofences obtained by both FFT-based KDE and traditional KDE are displayed in fig. 2.

For FFT-based KDE, the ratio of the number of the data points bounded by the geofence to that of all the generated data points is 80.7%. For traditional KDE, the ratio is 81.6%. This means both methods can guarantee that without violating the geofence, the probability of conflicts will not exceed $\alpha = 20\%$, and the geofence obtained by FFT-based KDE is tighter than traditional KDE.

In addition, for FFT-based KDE, the ratio of the number of cells bounded by the geofence to the total number of cells is 14.4%, while the ratio for traditional KDE is 15.2%. This also demonstrates the tightness of online evaluation of chance-constrained geofence through FFT-based KDE.

The Jaccard score compares members for two sets to see which members are shared and which are distinct. It's a measure of similarity for the two sets of data, with a range from 0% to 100%. The higher the percentage, the more

similar the two populations. Formally, for any two sets A and B, the Jaccard score is defined as

$$J(A, B) = \frac{|A \cap B|}{|A \cup B|} \tag{14}$$

where $|\cdot|$ is the cardinality of a set. The Jaccard score between the geofence obtained by FFT-based KDE and by traditional KDE is 94.1%. This illustrates that the chance-constrained geofences identified by both methods are almost the same.

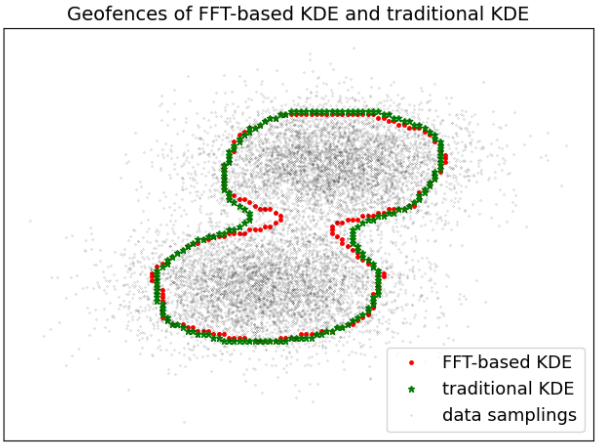

Fig. 2 Confidence level = 80%

2) Confidence level $\alpha = 90\%$

The chance-constrained geofences obtained by both FFT-based KDE and traditional KDE are displayed in fig. 3.

For FFT-based KDE, the ratio of the number of the data points bounded by the geofence to that of all the generated data points is 91.1%. For traditional KDE, the ratio is 91.3%. Thus, both methods can ensure that following the identified geofence lead to the conflict probability not exceeding 10%.

Also, for FFT-based KDE, the ratio of the number of cells bounded by the geofence to the total number of cells is 20.4%, while the ratio for traditional KDE is 21.3%. The geofence obtained by traditional KDE is more conservative than FFT-based KDE. Compared with confidence level $\alpha = 80\%$ in 1), the number of cells obtained from confidence level $\alpha = 90\%$ becomes larger to cover more sampled data points.

The Jaccard score between the geofence obtained by FFT-based KDE and traditional KDE is 95.2%, indicating the overlapping part of two geofences is very large.

3) Confidence level $\alpha = 95\%$

The chance-constrained geofences obtained by both FFT-based KDE and traditional KDE are displayed in fig. 4.

For FFT-based KDE, the ratio of the number of the data points bounded by the geofence to that of all the generated data points is 95.6%. For traditional KDE, the ratio is 96.1%. This ensures that either method can provide an accurate bound for flying safety.

In addition, for FFT-based KDE, the ratio of the number of cells bounded by the geofence to the total number of cells is 26.0%, while the ratio for traditional KDE is 26.9%, which shows FFT-based KDE provides a tighter bound.

Also, the Jaccard score between the geofence obtained by FFT-based KDE and by traditional KDE is 95.6%.

4) Confidence level $\alpha = 99.9999\%$

In real applications, for the safety guarantee of aviation, the confidence level $\alpha \geq 99.9999\%$. The number of data points is still $N = 10^4$, the number of grid points in each dimension is still $M = 128$. The chance-constrained geofences obtained by both FFT-based KDE and traditional KDE are displayed in fig. 5.

For FFT-based KDE, the ratio of the number of the data points bounded by the geofence to that of all the generated data points is 100%. In other words, all the generated data points have been bounded by the established geofence. For traditional KDE, as shown in fig. 5, the established geofence is more conservative than FFT-based KDE and therefore it can also bound all the generated data points.

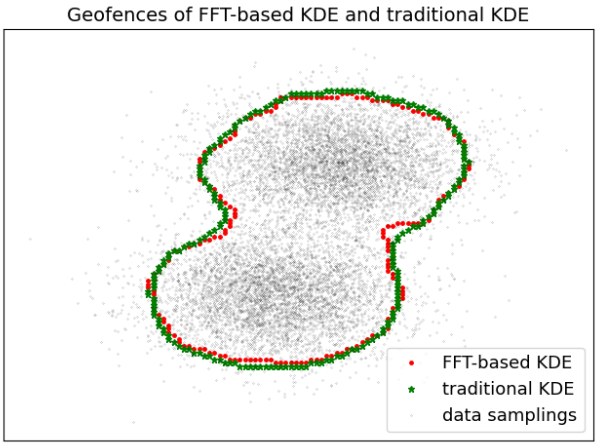

Fig. 3 Confidence level = 90%

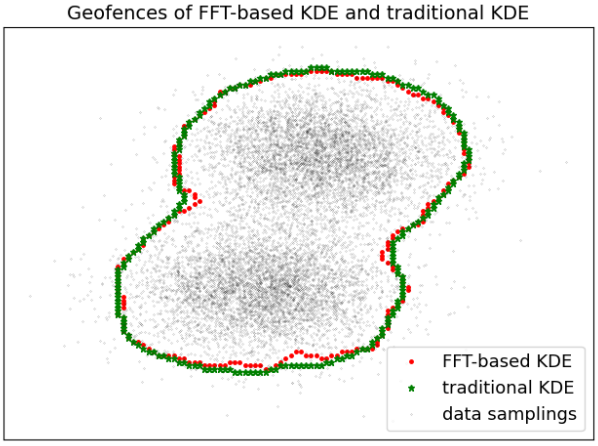

Fig. 4 Confidence level = 95%

In addition, about 63.7% of the total cells are bounded by the geofence obtained through FFT-based KDE. For traditional KDE, the ratio is 72.3%. This result is consistent with the observation that the area of the geofence from FFT-based KDE is smaller than that of traditional KDE.

Also, the Jaccard score between the geofence obtained by FFT-based KDE and by traditional KDE is 87.9%.

The comparisons between two methods are summarized in Table 1.

C. Evaluation time comparison in terms of data points N

In this part, we are going to make a comparison in terms of the evaluation time of online evaluation of chance-constrained geofence between FFT-based KDE and traditional KDE, with respect to the increasing number of data points N. The number of data points N ranges from 10^3 to 10^6. The number of grid points M in each dimension is fixed to be 128, and the confidence level α is fixed to be 95%.

As illustrated in fig. 6, FFT-based KDE greatly outperforms the traditional one in terms of the evaluation time. This demonstrates that the proposed algorithm of online evaluation of chance-constrained geofence using FFT-based KDE can run in an online fashion.

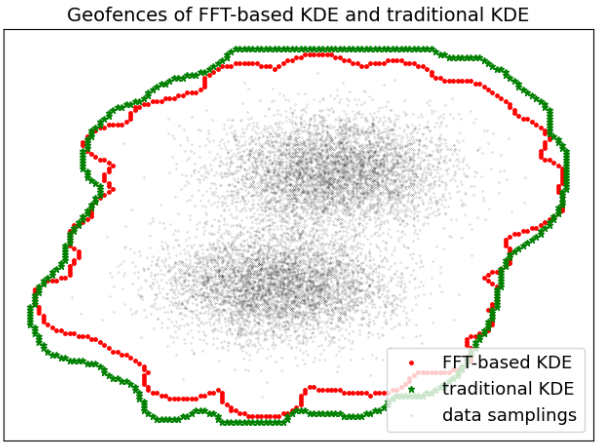

Fig. 5 Confidence level = 99.9999%

Table 1 Method comparisons

Confidence Level	Method	Ratio of Point	Ratio of Area	Jaccard Score
$\alpha = 80\%$	FFT-based	80.7%	14.4%	94.1%
	Traditional	81.6%	15.2%	
$\alpha = 90\%$	FFT-based	91.1%	20.4%	95.2%
	Traditional	91.3%	21.3%	
$\alpha = 95\%$	FFT-based	95.6%	26.0%	95.6%
	Traditional	96.1%	26.9%	
$\alpha = 99.9999\%$	FFT-based	100%	63.7%	87.9%
	Traditional	100%	72.3%	

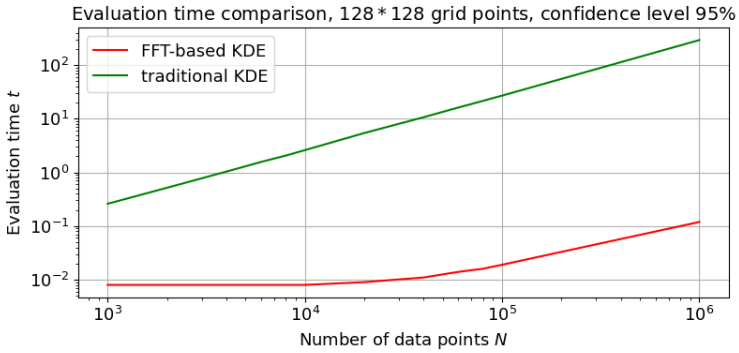

Fig. 6 Evaluation time comparison

V. Conclusions

How to ensure operation safety in high-density, dynamic and uncertain airspace environments in real time is a key challenge for the success of UAM. This paper introduces a concept called chance-constrained Geo-fences that can guarantee that the probability of potential conflicts is bounded and low. To efficiently evaluate the chance-constrained Geo-fences in an online fashion, a data-driven method is developed for any general empirical distribution.

In specific, we present an alternative way for kDE method to replace performing kernel evaluation on data points by that on grids. Further, FFT can be implemented to reduce computational complexity owing to the structure of

discrete convolution of kernel evaluation. Numerical study shows this indirect approach can dramatically increase the speed of computation. Based on the results of KDE evaluation, we propose an algorithm of online data-driven evaluation to capture chance-constrained geofence. The identification of chance-constrained geofence can help translate the data-driven uncertainty into deterministic constraints for the path planning of eVTOL aircraft in UAM applications. Numerical study demonstrates the evaluation of chance-constrained geofence can be achieved in an online fashion.

The chance-constrained geofence identified in this paper is not convex, which brings difficulty to the path planning of multi-agent systems in real applications. In the future, we are going to formulate a optimization-driven problem whose solution can provide a convex approximation for the chance-constrained geofence evaluated in this paper.

Acknowledgments

This work was supported by the National Science Foundation under Grants CMMI-2138612.

References

[1] L. Gipson, *Nasa embraces urban air mobility, calls for market study*, `https://www.nasa.gov/aero/nasa-embraces-urban-air-mobility`, Accessed: 2020-02-15, 2017.

[2] J. Holden and N. Goel, "Fast-forwarding to a future of on-demand urban air transportation," *San Francisco, CA*, 2016.

[3] N. Polaczyk, E. Trombino, P. Wei, and M. Mitici, "A review of current technology and research in urban on-demand air mobility applications," in *8th Biennial Autonomous VTOL Technical Meeting & 6th Annual Electric VTOL Symposium*, Jan. 2019.

[4] P. Wu, X. Yang, P. Wei, and J. Chen, "Safety assured online guidance with airborne separation for urban air mobility operations in uncertain environments," *IEEE Transactions on Intelligent Transportation Systems*, 2022.

[5] X. Yang and P. Wei, "Scalable multi-agent computational guidance with separation assurance for autonomous urban air mobility," *Journal of Guidance, Control, and Dynamics*, vol. 43, no. 8, pp. 1473–1486, 2020.

[6] Z. Zhou, J. Chen, and Y. Liu, "Optimized landing of drones in the context of congested air traffic and limited vertiports," *IEEE Transactions on Intelligent Transportation Systems*, vol. 22, no. 9, pp. 6007–6017, 2020.

[7] S. Kahne and I. Frolow, "Air traffic management: Evolution with technology," *IEEE Control Systems*, vol. 16, no. 4, pp. 12–21, 1996.

[8] M. Stevens and E. Atkins, "Geofence definition and deconfliction for uas traffic management," *IEEE Transactions on Intelligent Transportation Systems*, 2020.

[9] G. Zhu and P. Wei, "Pre-departure planning for urban air mobility flights with dynamic airspace reservation," in *AIAA Aviation 2019 Forum*, 2019, p. 3519.

[10] J. M. Hoekstra, R. N. van Gent, and R. C. Ruigrok, "Designing for safety: The 'free flight'air traffic management concept," *Reliability Engineering & System Safety*, vol. 75, no. 2, pp. 215–232, 2002.

[11] H. A. Blom and G. Bakker, "Safety evaluation of advanced self-separation under very high en route traffic demand," *Journal of Aerospace Information Systems*, vol. 12, no. 6, pp. 413–427, 2015.

[12] L. Cheng, H. Wen, and D. Jin, "Uncertain parameters analysis of powered-descent guidance based on chebyshev interval method," *Acta Astronautica*, vol. 162, pp. 581–588, 2019.

[13] J. P. Hespanha, H. H. Kizilocak, and Y. S. Ateskan, "Probabilistic map building for aircraft-tracking radars," in *Proceedings of the 2001 American Control Conference.(Cat. No. 01CH37148)*, IEEE, vol. 6, 2001, pp. 4381–4386.

[14] D. Althoff, D. Wollherr, and M. Buss, "Safety assessment of trajectories for navigation in uncertain and dynamic environments," in *2011 IEEE International Conference on Robotics and Automation*, IEEE, 2011, pp. 5407–5412.

[15] X. Yang, L. Deng, J. Liu, P. Wei, and H. Li, "Multi-agent autonomous operations in urban air mobility with communication constraints," in *AIAA Scitech 2020 Forum*, 2020, p. 1839.

[16] B. Du, J. Chen, D. Sun, S. G. Manyam, and D. W. Casbeer, "Uav trajectory planning with probabilistic geo-fence via iterative chance-constrained optimization," *IEEE Transactions on Intelligent Transportation Systems*, 2021.

[17] P. Wu, H. Wen, T. Chen, and D. Jin, "Model predictive control of rigid spacecraft with two variable speed control moment gyroscopes," *Applied Mathematics and Mechanics*, vol. 38, no. 11, pp. 1551–1564, 2017.

[18] L. Blackmore, M. Ono, and B. C. Williams, "Chance-constrained optimal path planning with obstacles," *IEEE Transactions on Robotics*, vol. 27, no. 6, pp. 1080–1094, 2011.

[19] L. Blackmore, M. Ono, A. Bektassov, and B. C. Williams, "A probabilistic particle-control approximation of chance-constrained stochastic predictive control," *IEEE transactions on Robotics*, vol. 26, no. 3, pp. 502–517, 2010.

[20] P. Wu, L. Li, J. Xie, and J. Chen, "Probabilistically guaranteed path planning for safe urban air mobility using chance constrained rrt," in *AIAA Aviation 2020 Forum*, 2020, p. 2914.

[21] P. Lathrop, B. Boardman, and S. Martınez, "Distributionally safe path planning: Wasserstein safe rrt," *IEEE Robotics and Automation Letters*, vol. 7, no. 1, pp. 430–437, 2021.

[22] W. Dai, B. Pang, and K. H. Low, "Conflict-free four-dimensional path planning for urban air mobility considering airspace occupancy," *Aerospace Science and Technology*, p. 107 154, 2021.

[23] P. Wu, J. Xie, and J. Chen, "Safe path planning for unmanned aerial vehicle under location uncertainty," in *2020 IEEE 16th International Conference on Control & Automation (ICCA)*, IEEE, 2020, pp. 342–347.

[24] M. P. Wand and M. C. Jones, *Kernel smoothing*. CRC press, 1994.

[25] J. Fan and J. S. Marron, "Fast implementations of nonparametric curve estimators," *Journal of computational and graphical statistics*, vol. 3, no. 1, pp. 35–56, 1994.